Received: 19 May 2022 | Revised: 21 July 2022 | Accepted: 15 October 2022

IET Generation, Transmission & Distribution

DOI: 10.1049/gtd2.12660

The Institution of Engineering and Technology WILEY

ORIGINAL RESEARCH

Nonlinear finite-time control of hydroelectric systems via a novel sliding mode method

Runfan Zhang[1] | **Xinyi Ren**[1] | **Md. Apel Mahmud**[2] | **Huanhuan Li**[3]

[1]School of Electrical Engineering, Xi'an Jiaotong University, Xi'an, Shaanxi, China

[2]Electrical Power and Energy Systems Research Lab, School of Engineering, Deakin University, Geelong, Victoria, Australia

[3]School of Water and Environment, Chang'an University, Xi'an, Shaanxi, China

Correspondence
School of Water and Environment, Chang'an University, Xi'an 710054, Shaanxi, China.
Email: huanhuanli@chd.edu.cn

Funding information
National Natural Science Foundation of China, Grant/Award Number: 52207135; China Postdoc Council of 2021 International Postdoctoral Exchange Fellowship Program (Talent-Introduction Program), Grant/Award Number: YJ20210153; Fundamental Research Funds for the Central Universities, Grant/Award Number: xzy012022061

Abstract

A nonlinear finite-time sliding mode control is proposed in this paper for the governing of complex hydroelectric systems with the finite/fixed setting time. The proposed control method is derived from the finite-time stability and sliding mode control theories. The finite settling time is calculated and bounded, not depending on the initial conditions of the system. The solution trajectory of the controlled hydroelectric system can reach the sliding manifold in a fixed settling time, regardless of initial values. Based on the Lyapunov theory, the controlled hydroelectric system also converges to a reference state within the fixed settling time. A simulation of a high-dimensional hydroelectric system verifies the feasibility of the proposed method. In addition, a comparison between the proposed method and the conventional PID method demonstrates the advantages of the proposed method in the shorter settling time and smaller overshoot. The proposed control method allows for the design of a flexible controller and provides an improvement in dynamic performance.

1 | INTRODUCTION

Hydroelectricity is a clean, efficient, and reliable form of energy whose contribution to greenhouse gas emissions is negligible in comparison with fossil fuels [1, 2]. Century-developed hydro turbines and units make the modern huge hydro-power plants generate an amount of electricity among the whole power system [3, 4]. However, the large hydroelectric scheme casts difficulties on its governing systems, since any possible fault could result in the failure of the whole power system. Thus, the control system for the hydroelectric plants is of significance. Literature has been concerned about the stable operation conditions of diverse hydroelectric systems [5–7]. The large hydroelectric system is a complex system and difficult to be controlled, incorporating the electric system, hydro turbine system, mechanical system, and control system [8]. The hydroelectric system, coupled with the above subsystems, shows varied dynamic behaviours. As a result, the control of the hydroelectric system turns out to be a difficult issue. In addition, the small/micro-hydroelectric plants, as a kind of distributed resource, require the control system to be accurate and flexible for the possibility of the islanded operation [9].

Conventional control strategies have been applied to the hydroelectric system such as PID controllers [10] and its varied methods [11], and feedback controller [12]. These controllers are normally tuned based on linear transfer functions. However, hydroelectric systems are highly nonlinear, time-variant, and multi-variable. Any controlling law designed based on a linearized representation is a compromise [13]. For this reason, state-of-the-art methods have been introduced to hydroelectric systems, for instance, sliding mode control [14–17], fuzzy control [18, 19], predictive control [20, 21], and so on.

Most of the above-mentioned control systems for the hydroelectric system are derived from asymptotic stability theories, with the convergence process of the closed-loop system at most exponential and the containment tracking errors decreasing to zero with infinite settling time [22]. Such a control scheme no longer meets the higher requirements of large hydroelectric systems. In addition, the finite-time control method ensures the system converges within a finite settling time. The

finite-time controller has a faster convergence rate, higher precision, and more robustness to uncertainties [23–25]. Many remarkable outcomes have been reported about the finite-time stability theories, for example, the finite-time stability for linear time-delay systems [26], the necessary and sufficient conditions for the finite-time stability of systems [27], and the global finite-time stability theory [28]. The above literature presents simple feedback control strategies for governing systems. Besides, other advanced control methods based on finite-time stability theories have also been reported such as the finite-time feedback control [29, 30], sliding model control [31], H-infinity control [32, 33], and fault-tolerant control [34, 35]. A fixed-time adaptive backstepping control was successfully implemented for an anti-synchronization problem with good performance in the elimination of singular problem [36]. To control a high-order nonlinear system, an adaptive neural fixed-time tracking control was proposed with overcoming the design difficulty that appeared in the non-strict feedback structure [37]. A novelty finite-region H∞ asynchronous control scheme was developed for the transient behaviour of a class of two-dimensional Markov jump systems [38]. A new robust sliding mode control was designed for a class of discrete conic-type nonlinear systems with time delays and uncertain parameters with a better performance and disturbance attenuation level [39]. To govern nonlinear Markov jump systems, an asynchronous output feedback controller was proposed with both stochastically finite-time bounded and satisfying the attenuation condition of predefined finite-time H∞ performances[40]. Invoked by the above novelty literature, a different technique is implemented in this paper, in which the sliding surface is designed with a unique function ensuring fixed-time stability. All the existing literature illustrates the possibility of the implementation of the finite-time controllers on hydroelectric systems whereas the convergence time of the finite-time control method depends on the initial condition of the systems. As a result, the control laws with fixed-time stability and guaranteed settling time regardless of the initial states were proposed in ref. [41].

From the motivation of the above discussions, this paper proposes a finite-time sliding mode control method to stabilize the complex and nonlinear hydroelectric system shown in Figure 1. The sliding mode control law is derived using the finite-time stability theory and the upper bound of the settling time is also found in this work. It can be further proved that the settling time is independent of initial states. As a higher-order sliding mode controller is proposed to achieve a fixed-time convergence with higher accuracy [42], the stability of the proposed method and the finite and fixed settling time are obtained through the Lyapunov method. The main contributions of this paper are:

(1) A new sliding mode-based finite-time control scheme for the nonlinear hydroelectric systems is designed;
(2) The stability of the proposed controller and its bounded settling time are analysed and calculated from the viewpoint of Lyapunov theory;
(3) The feasibility of the proposed controller for the hydroelectric system is successfully validated.

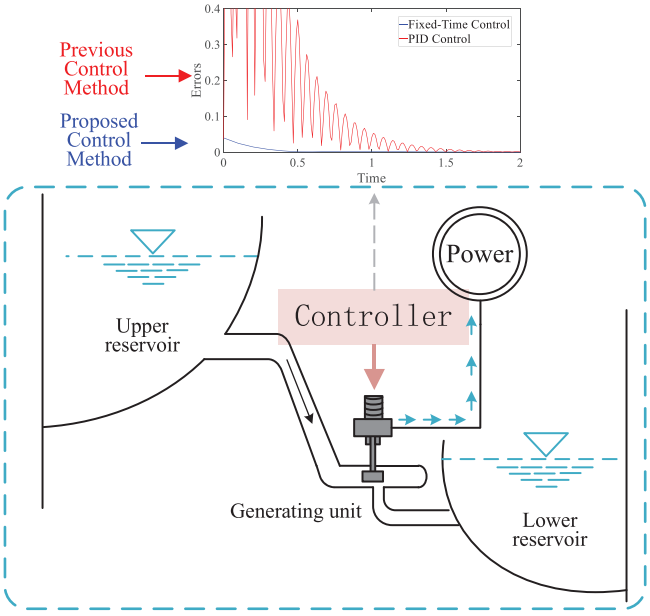

FIGURE 1 Diagram of hydroelectric system and the comparison between the previous PID control method and the proposed control method in this paper

Compared with other sliding mode methods, the sliding mode surface proposed in this paper, first of all, has a higher-order design.

Secondly, the sliding mode control is fixed-time stability based. Finally, the unique sliding mode surface ensures the fixed and finite setting time can be theoretically found.

The rest parts of the paper are organized as follows. In Section 2, two basic inequality lemmas are illustrated. The finite-time control method is proposed in Section 3. Section 4 presents the results from the application of the proposed controller on the nonlinear hydroelectric system. Section 5 summarizes the main findings while Appendix A provides the proofs for the theorem proposed in Section 3.

2 | PRELIMINARIES

The sliding mode control for hydroelectric systems is proposed based on the finite/fixed time stability. Some preliminaries including the definitions and concepts are introduced as follows based on the conventions in the literature. There is such a system as:

$$\dot{x} = f(t, x), x(0) = x_0, \tag{1}$$

where $x \in \mathfrak{R}^n$ and $f : \mathfrak{R}_+ \times \mathfrak{R}^n \to \mathfrak{R}^n$ is an either continuous or discontinuous nonlinear function. Assume the equilibrium point of Equation (1) is $x(0) = 0$. Many remarkable concepts of the finite-time stability are proposed during the last years. The conventional definition of the finite-time stability is illustrated as follows.

Definition 1. ([43]): The equilibrium point of Equation (1) is so-called to be globally finite-time stable if it is globally asymptotically stable and any solution $x(t, x(0))$ of Equation (1) reaches the equilibria at some finite-time moment, i.e. $x(t, x(0)) = 0, \forall t \geq T(x_0)$, where $T : \mathfrak{R}^n \to \mathfrak{R}_+ \cup \{0\}$ is the setting-time function.

Furthermore, a concept of fixed-time stability was defined as below.

Definition 2. ([44]): The equilibrium point of Equation (1) is so-called to be globally fixed-time stable if it is globally finite-time stable and the settling time function $T(x(0))$ is bounded, i.e. $\exists T_{\max} > 0 : T(x(0)) \leq T_{\max}, \forall x(0) \in \mathfrak{R}^n$.

Then, two inequalities are introduced for the stability analysis in Section 3.

Lemma 1. *([45]): If $x_i > 0,\ 0 < q \leq 1$, then there is the following inequality:*

$$\left(\sum_{i=1}^{n} x_i\right)^q \leq \sum_{i=1}^{n} x_i^q. \tag{2}$$

Lemma 2. *([46]): If $x_i > 0,\ q > 1$, then there is the following inequality:*

$$\left(\sum_{i=1}^{n} x_i\right)^q \leq n^{q-1} \sum_{i=1}^{n} x_i^q. \tag{3}$$

3 | FINITE-TIME SLIDING MODE CONTROL SCHEME

A finite-time control method is proposed based on the high-order sliding mode strategy. The proposed method enables the controlled system to reach the reference in a finite settling time. The bound of the time, regardless of the initial values, is also found. Here, the system model can be represented as:

$$\dot{\mathbf{x}} = \mathbf{f}(\mathbf{x}) + \mathbf{g}(\mathbf{x})\mathbf{u} + \mathbf{w}(t), \tag{4}$$

where $\mathbf{x} \in \mathfrak{R}^n$, $\mathbf{u} \in \mathfrak{R}^n$, $\mathbf{f}(\cdot) \in \mathfrak{R}^n$ are the state vector, control vector and nonlinear function, respectively; $\mathbf{g}(\cdot) \in \mathfrak{R}^{n\times n}$ is the nonlinear function which satisfies $rank(\mathbf{g}(\cdot)) = n$ and $\mathbf{g}(\cdot) \neq \mathbf{0}$; $\mathbf{w}(t)$ is the system disturbance satisfying $|\mathbf{w}(t)| \leq M$; and M is the disturbance bound.

The system error can be selected as:

$$\mathbf{e} = \mathbf{x} - \mathbf{x}_r, \tag{5}$$

where $\mathbf{e} \in \mathfrak{R}^n$, $\mathbf{e} = [e_1, \ldots e_i, \ldots e_n]^T$; $\mathbf{x}_r \in \mathfrak{R}^n$, $\mathbf{x}_r = [x_{r1}, \ldots x_{ri}, \ldots x_{rn}]^T$ are the reference states.

The sliding surface of the finite-time control method is designed as follows:

$$\mathbf{S} = \mathbf{e} + \eta \mathbf{sgn}(\mathbf{e}) \int_{t_0}^{t} \left(\sum_{i=1}^{n} |e_i|^{2\alpha} + 1\right)^{\frac{3}{2}} \sum_{i=1}^{n} |e_i|^{1-\alpha} d\tau, \tag{6}$$

where $\eta \in \mathfrak{R}^{n\times n}$ depicts the convergence rate which is positive definite and diagonal matrix; $\mathbf{sgn}(\mathbf{x})$ is a $n \times 1$ signum function with sgn(·)-vector; and $0 < \alpha < 1$ is the sliding surface parameter.

The differentiation of Equation (6) gives Equation (7),

$$\begin{aligned}\dot{\mathbf{S}} = \dot{\mathbf{e}} &+ \eta \mathbf{sgn}(\mathbf{e}) \left(\sum_{i=1}^{n} |e_i|^{2\alpha} + 1\right)^{\frac{3}{2}} \sum_{i=1}^{n} |e_i|^{1-\alpha} \\ &+ 2\eta \boldsymbol{\delta}(\mathbf{e}) \int_{t_0}^{t} \left(\sum_{i=1}^{n} |e_i|^{2\alpha} + 1\right)^{\frac{3}{2}} \sum_{i=1}^{n} |e_i|^{1-\alpha} d\tau \\ = \mathbf{f}(\mathbf{x}) &+ \mathbf{g}(\mathbf{x})\mathbf{u} + \mathbf{w}(t) - \dot{\mathbf{x}}_r \\ &+ \eta \mathbf{sgn}(\mathbf{e}) \left(\sum_{i=1}^{n} |e_i|^{2\alpha} + 1\right)^{\frac{3}{2}} \sum_{i=1}^{n} |e_i|^{1-\alpha} \\ &+ 2\eta \boldsymbol{\delta}(\mathbf{e}) \int_{t_0}^{t} \left(\sum_{i=1}^{n} |e_i|^{2\alpha} + 1\right)^{\frac{3}{2}} \sum_{i=1}^{n} |e_i|^{1-\alpha} d\tau,\end{aligned} \tag{7}$$

where $\boldsymbol{\delta}(\mathbf{e})$ is a $n \times 1$ Dirac function vector whose engineering application can be found in ref. [47] (Chapter 3). In Equation (7), assuming that the system reference (x_r) is constant. Thus we will have $\dot{\mathbf{x}}_r = 0$. In this case, the equivalent controller ensuring the sliding surface to satisfy $\dot{\mathbf{S}} = \mathbf{0}$, can be obtained as in Equation (8).

$$\begin{aligned}\mathbf{u}_{eq} = -\mathbf{g}^{-1}(\mathbf{x}) \Bigg[&\mathbf{f}(\mathbf{x}) + M - \dot{\mathbf{x}}_r \\ &+ \eta \mathbf{sgn}(\mathbf{e}) \left(\sum_{i=1}^{n} |e_i|^{2\alpha} + 1\right)^{\frac{3}{2}} \sum_{i=1}^{n} |e_i|^{1-\alpha} \\ &+ 2\eta \boldsymbol{\delta}(\mathbf{e}) \int_{t_0}^{t} \left(\sum_{i=1}^{n} |e_i|^{2\alpha} + 1\right)^{\frac{3}{2}} \sum_{i=1}^{n} |e_i|^{1-\alpha} d\tau \Bigg].\end{aligned} \tag{8}$$

$$\begin{aligned}\mathbf{u}_s = -\mathbf{g}^{-1}(\mathbf{x}) \big[&\varepsilon \mathbf{sgn}^T(\mathbf{S}) E_n \mathbf{S}_{2-\beta} + \zeta \mathbf{sgn}^T(\mathbf{S}) E_n \mathbf{S}_{\text{abs}} \\ &+ \sigma \mathbf{sgn}^T(\mathbf{S}) E_n \mathbf{S}_{\beta} \big].\end{aligned} \tag{9}$$

$$\begin{aligned}\mathbf{u} = \mathbf{u}_{\text{eq}} + \mathbf{u}_s = \\ &- \mathbf{g}^{-1}(\mathbf{x})\left[\mathbf{f}(\mathbf{x}) + M\right. \\ &+ \eta \mathbf{sgn}(\mathbf{e})\left(\sum_{i=1}^{n} |e_i|^{2\alpha} + 1\right)^{\frac{3}{2}} \sum_{i=1}^{n} |e_i|^{1-\alpha} \\ &+ 2\eta\delta(\mathbf{e}) \int_{t_0}^{t} \left(\sum_{i=1}^{n} |e_i|^{2\alpha} + 1\right)^{\frac{3}{2}} \sum_{i=1}^{n} |e_i|^{1-\alpha} \mathrm{d}\tau \\ &+ \varepsilon \mathbf{sgn}^T(\mathbf{S}) E_n \mathbf{S}_{2-\beta} + \zeta \mathbf{sgn}^T(\mathbf{S}) E_n \mathbf{S}_{\text{abs}} \\ &\left. + \sigma \mathbf{sgn}^T(\mathbf{S}) E_n \mathbf{S}_{\beta}\right]. \end{aligned} \tag{10}$$

Then, we also need a switching controller $\mathbf{u}_s$ to enforce the system on the sliding surface, as Equation (9) where

$$\mathbf{S}_{2-\beta} = \left[|s_1|^{2-\beta}, |s_2|^{2-\beta}, \ldots |s_i|^{2-\beta}, \ldots |s_n|^{2-\beta}\right]^T, \tag{11}$$

$$\mathbf{S}_{abs} = \left[|s_1|, |s_2|, \ldots |s_i|, \ldots |s_n|\right]^T, \tag{12}$$

$$\mathbf{S}_{\beta} = \left[|s_1|^{\beta}, |s_2|^{\beta}, \ldots |s_i|^{\beta}, \ldots |s_n|^{\beta}\right]^T, \tag{13}$$

and $0 < \beta < 1$; E_n is an $n \times n$ unit matrix, ε, ζ, and σ are the switching control parameters which need to be designed. Combining the equivalent controller (8) with that of the switching controller (9) and substituting the disturbance by its maximum estimated value M will give the finite-time controller as in Equation (10).

Theorem 1 and 2 provide the stability of the proposed control method. Theorem 1 gives the finite-time stability of the controlled system and the settling time. Then, Theorem 2 finds the bound of the settling time and proves that the bound is independent of the initial values.

Theorem 1. *Implementation of the proposed finite-time controller (10) in the system (4), as long as* $\zeta^2 < 4\sigma\varepsilon n^{-\frac{1-\beta}{2}}$, $\epsilon > 0$, $\zeta > 0$ *and* $\sigma > 0$, *then the system (4) is with the finite-time stability, and the settling time is shown in Equation (14), where* $V(\cdot)$ *and* $L(\cdot)$ *are selected Lyapunov functions.*

$$\begin{aligned} T_x \le \frac{1}{\eta\alpha} \frac{(2V(t_s))^{\frac{\alpha}{2}}}{\sqrt{(2V(t_s))^{\alpha} + 1}} + \frac{2}{(1-\beta)\sqrt{4\sigma\varepsilon n^{-\frac{1-\beta}{2}} - \zeta^2}} \\ \times \arctan \frac{2\varepsilon n^{-\frac{1-\beta}{2}} (2L(t_0))^{\frac{1-\beta}{2}} + \zeta}{\sqrt{4\varepsilon\sigma n^{-\frac{1-\beta}{2}} - \zeta^2}}, \end{aligned} \tag{14}$$

Theorem 2. *The finite settling time in Equation (14) is bounded by:*

$$T_{x\max} = \frac{1}{\eta\alpha} + \frac{\pi}{(1-\beta)\sqrt{4\sigma\varepsilon n^{-\frac{1-\beta}{2}} - \zeta^2}}. \tag{15}$$

The proofs of Theorem 1 and 2 can be found in Appendix A.

Obviously, Equation (15) is independent of the initial values of the system. The system, governed by the proposed fixed-time controller, always reaches the reference within the fixed settling time.

The design procedure of the proposed sliding mode control can be summarized below.

(1) Designing the sliding surface (6)
(2) Designing the equivalent controller (8)
(3) Designing the switching controller (9)
(4) Following Theorem 1 to calculate the control parameters $\epsilon > 0, \zeta > 0$ and $\sigma > 0$
(5) Based on Equation (14) in Theorem 1 and Equation (15) in Theorem 2 to find the finite settling time T_x, and its bound $T_{x\max}$

Remark 1. The introduction of symbolic function in the sliding surface enhances the sliding surface converging into equilibrium. For the sliding surface, the equilibrium is $\mathbf{S} = 0$. Normally, the sliding surface is designed as $\mathbf{S} = 0$ the dynamic (1) will reach $x = 0$. With the symbolic function of the sliding surface, both the sliding surface and state x converge to the equilibrium faster, and the closer to the equilibrium point the faster the convergence. As a result, finite-time convergence can be achieved. In addition, the enhancement of robustness of the controlled system can be provided based on the design of the sliding surface with the symbolic function. The introduction of symbolic function in the sliding surface has already been implemented in many reports [48].

4 | FIXED-TIME CONTROL OF THE HYDROELECTRIC SYSTEM

The proposed control method is verified with the following hydroelectric power system in four different scenarios.

4.1 | Case study A

Considering the voltage behind the transient reactance of a synchronous generator E'_q in the hydroelectric system model described in the ref. [49] the seven-dimensional hydroelectric

system model is obtained as:

$$\begin{cases} \dot{x}_1 = x_2 + u_1 + w_1(t) \\ \dot{x}_2 = x_3 + u_2 + w_2(t) \\ \dot{x}_3 = -a_0 x_1 - a_1 x_2 - a_2 x_3 + y + u_3 + w_3(t) \\ \dot{\delta} = \omega_B(\omega - 1) + u_\delta + w_\delta(t) \\ \dot{\omega} = \dfrac{1}{T_{ab}}[m_t - P_e - D(\omega - 1)] + u_\omega + w_\omega(t) \\ \dot{E}'_q = -\dfrac{\omega_B}{T_{d0'}} \dfrac{x_{d\Sigma}}{x'_{d\Sigma}} E'_q + \dfrac{\omega_B}{T_{d0'}} \dfrac{x_{d\Sigma} - x'_{d\Sigma}}{x'_{d\Sigma}} V_s \cos\delta \\ \qquad + \dfrac{\omega_B}{T_{d0'}} E_f + u_{E'_q} + w_{E'_q}(t) \\ \dot{y} = \dfrac{1}{T_y}\left(-y + u_y\right) + w_y(t) \end{cases} \tag{16}$$

where $P_e = \frac{E'_q V_s}{x'_{d\Sigma}} \sin\delta + \frac{V_s^2 (x'_{d\Sigma} - x_{q\Sigma})}{2 x'_{d\Sigma} x_{q\Sigma}} \sin 2\delta$, $\omega_B = 314$ rad/s, $x'_d = 0.34, x_q = 0.66, T_{d0'} = 0.54, T_y = 0.1,, x'_{d\Sigma} = 1.15, x'_{q\Sigma} = 1.474$, $V_s = 1.0$, $a_0 = 24$, $a_2 = 3$, $b_0 = 24$, $b_1 = 33.6$, $b_2 = 3, b_3 = -1.4$, and $M = 0.003$. These parameters are derived from ref. [49]. In, Equation (16), $\mathbf{x} = [x_1, x_2, x_3, \delta, \omega, E'_q, y]^T$.

$\mathbf{w} = [w_1, w_2, w_3, w_\delta, w_\omega, w_{E'_q}, w_y]^T$ are the disturbances, $\mathbf{u} = [u_1, u_2, u_3, u_\delta, u_\omega, u_{E'_q}, u_y]^T$ are control inputs, $\mathbf{G}(\mathbf{x}) = I_7$, and $\mathbf{f}(\mathbf{x})$ is shown below.

$$\mathbf{f}(\mathbf{x}) = \begin{cases} \dot{x}_1 = x_2 \\ \dot{x}_2 = x_3 \\ \dot{x}_3 = -a_0 x_1 - a_1 x_2 - a_2 x_3 + y \\ \dot{\delta} = \omega_B(\omega - 1) \\ \dot{\omega} = \dfrac{1}{T_{ab}}[m_t - P_e - D(\omega - 1)] \\ \dot{E}'_q = -\dfrac{\omega_B}{T_{d0'}} \dfrac{x_{d\Sigma}}{x'_{d\Sigma}} E'_q + \dfrac{\omega_B}{T_{d0'}} \dfrac{x_{d\Sigma} - x'_{d\Sigma}}{x'_{d\Sigma}} V_s \cos\delta \\ \qquad + \dfrac{\omega_B}{T_{d0'}} E_f + w_{E'_q}(t) \\ \dot{y} = -\dfrac{y}{T_y}. \end{cases} \tag{17}$$

According to Equation (16) and designing the corresponding controller based on Equation (10) with $\mathbf{x}_{r0} = [0, 0, 0, 0, 0, 0, 0]^T$, we are able to obtain the results of the controlled hydroelectric system as Figure 2(a).

Remark 2. In Figure 2(a), the system seems to reach the reference state before the settling time T_x as the system state to the reference state with a very small error after $t = 2$. However, the system absolutely reaches the reference state after T_x. In addition, $T_{x\max}$ can be obtained without the system initial values.

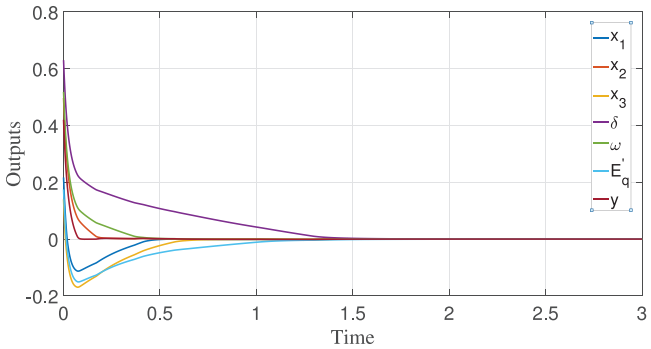

(a) The controlled system with the original point in Case Study A.

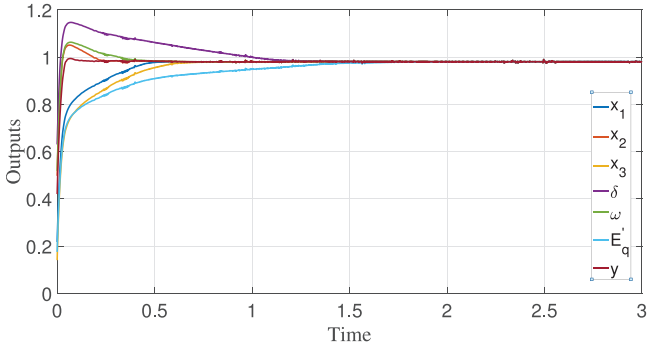

(b) The controlled system with the reference in Case Study A.

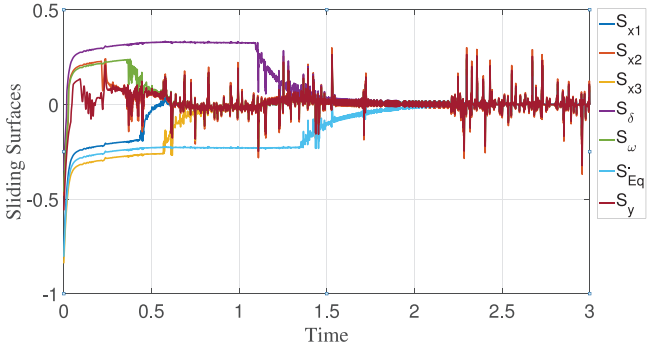

(c) The sliding surface of the controller with the reference in Case Study A.

FIGURE 2 The outputs and sliding surface of the hydro turbine system controlled by the fixed-time controller in case study A

In practice, the system is allowed to run beyond a small neighbouring region of the reference. In this case, $L(t_s)$ and $L(t_x)$ in Equations (A9) and (A18) are no longer zero and one just needs to substitute the bound of the neighbouring region into the corresponding Lyapunov function to calculate the finite and fixed settling time, respectively. In this case, the calculated time is smaller than the time in Equations (14) and (15).

The controller (10) enables the system (4) to reach any possible reference state. The following simulation shows the results of the different reference state $\mathbf{x}_{r1} = [0.98, 0.98, 0.98, 0.98, 0.98, 0.98, 0.98]^T$. From Figure 2(b), the system reaches to the references within a fixed settling time. In addition the sliding surfaces in this case study with $\mathbf{x}_{r1}$ are shown in Figure 2(b).

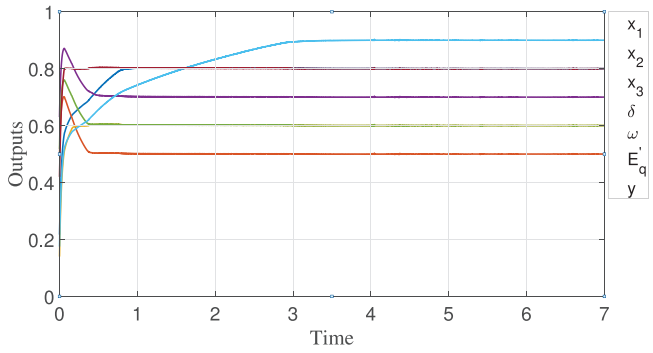

(a) The controlled system with reference in Case Study B.

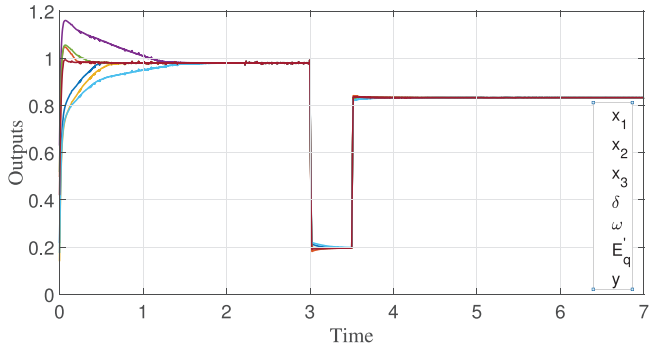

(b) The controlled system with a fault $\mathbf{x}_{r2}$ in Case Study C.

FIGURE 3 The outputs of the controlled system with the reference and fault $\mathbf{x}_{r2}$

4.2 | Case study B

In addition, the controller can also make a system to reach a divergent reference such as $\mathbf{x}_{r2} = [0.8, 0.5, 0.6, 0.7, 0.6, 0.9, 0.8]^T$. The result is shown in Figure 3(a). Although each reference is different, the controller ensures the system to reach the reference.

4.3 | Case study C

The controller (10) also ensures the system is stabilized to the reference even though faults exist in the system. The following simulation shows that the controller can also enable the system to be stable when a fault occurs at $t = 3$ and after $t = 3.5$, the system recovers from the faults. In the simulation, a very low point state represents the existence of the fault and the system cannot maintain the original state after the system recovers. The result is illustrated in Figure 3(b).

From Figure 2(b), when the system recovers from the fault after a few seconds, the controlled system reaches the reference states verifying the robustness of the proposed control method.

4.4 | Case study D

The proposed control method offers an advantage over the traditional PID control method. The following comparison simulation in Figure 4 supports the point. The PID controller is designed based on ref. [50]. In the simulation, the system shares the same initial values and parameters shown in the previous cases. The PID control parameters are taken from ref. [50] and the fixed-time control parameters are the same as in previous cases. The results are presented by the second norm of the errors in Figure 4.

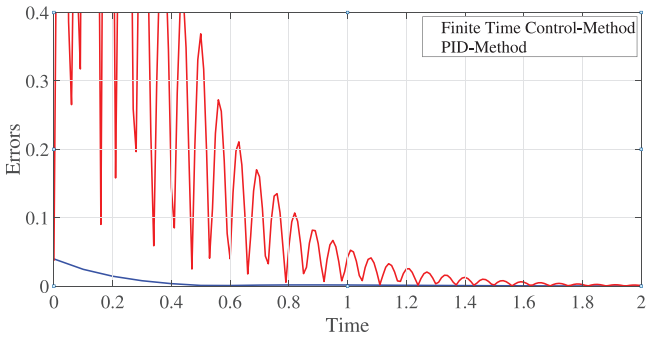

FIGURE 4 The outputs of the PID control method and the fixed-time control method in case study D

TABLE 1 Settling time of each case

Cases	T_x	$T_{x\max}$
Case study A $\mathbf{x}_{r0}$	2.9036	27.833
Case study A $\mathbf{x}_{r1}$	2.9685	27.833
Case study B $\mathbf{x}_{r2}$	4.1803	27.833

Figure 4 shows that the application of the finite-time control method to the hydroelectric system can improve its dynamic response and reduce the overshoot and settling time. Thus, the method in this paper is able to control a nonlinear system with expected performance.

Remark 3. From Equation (14), it rationally obtains the finite settling time for the controlled hydroelectric power system in different scenarios, which are shown in Table 1. Based on Equation (14), the finite settling time is dependent on the initial values, thus, there are varying in different cases. While, since the fixed settling time is regardless of the initial values, thus the fixed settling time of the different cases is the same shown as in Table 1.

5 | CONCLUSION

Based on sliding mode control theory, a finite-time control method was designed in the paper to govern a complex nonlinear hydroelectric system. Owing to this finite-time control, the settling time is bounded regardless of the initial values of the system. The stability of the controlled system was proved by the Lyapunov theorem. The finite and fixed settling times have been calculated for the performance evaluation. In addition to this, a method, aiming to calculate the settling time to reach an arbitrary neighbour region, has also been discussed. To verify

the proposed control method, a high-dimensional hydroelectric system was introduced in this paper. The numerical results have shown that the fixed-time control enables the nonlinear hydroelectric system to reach different references within its settling time. To further depict the control performance, the results from the proposed finite-time controller were compared with the conventional PID control. It has been demonstrated that the application of the fixed-time controller significantly improves the dynamic response of the hydroelectric system. The primary advantages of the finite-time controller include smooth treatment, less overshoot, and a short settling time in the response relative to the conventional PID controller. Another advantage is that the performance of the fixed-time controller is anticipated in the design stage without initial values.

AUTHOR CONTRIBUTIONS

Runfan Zhang: Conceptualization, data curation, formal analysis, funding acquisition, methodology, writing - original draft, writing - review and editing. Xinyi Ren: Investigation, validation, writing - original draft, writing - review and editing. Md Apel Mahmud: Investigation, validation, writing - review and editing. Huanhuan Li : Project administration, resources, software, supervision, visualization.

ACKNOWLEDGMENTS

This work is supported by the National Natural Science Foundation of China No. 52207135; the China Postdoc Council of 2021 International Postdoctoral Exchange Fellowship Program (Talent-Introduction Program) No. YJ20210153; the Fundamental Research Funds for the Central Universities No. xzy012022061.

CONFLICT OF INTEREST

The authors declare no conflict of interest.

DATA AVAILABILITY STATEMENT

The data that support the findings of this study are available from the corresponding author upon reasonable request.

ORCID

Runfan Zhang https://orcid.org/0000-0002-4696-6260
Md. Apel Mahmud https://orcid.org/0000-0002-5302-5338

REFERENCES

1. Lin, Y., Qiao, Y., Lu, Z.: Long-term generation scheduling for renewable-dominant systems concerning limited energy supporting capability of hydrogeneration. IET Gener. Transm. Distrib. 16(1), 57–70 (2022)
2. Li, H., Zhang, R., Mahmud, M.A., Hredzak, B.: A novel coordinated optimization strategy for high utilization of renewable energy sources and reduction of coal costs and emissions in hybrid hydro-thermal-wind power systems. Appl. Energy 320, 119019 (2022)
3. Bremond, J., Vuillerod, G.: The hydraulic turbines of the three gorges dam. Houille Blanche 3, 46–50 (1999)
4. Du, M., Huang, Y., Liu, J., Wu, G., Jawad, S.: CVAR-based generation expansion planning of cascaded hydro-photovoltaic-pumped storage system with uncertain solar power considering flexibility constraints. IET Gener. Transm. Distrib. 15(21), 2953–2966 (2021)
5. Zhang, L., Wu, Q., Ma, Z., Wang, X.: Transient vibration analysis of unit-plant structure for hydropower station in sudden load increasing process. Mech. Syst. Sig. Process. 120, 486–504 (2019)
6. Yu, X., Yang, X., Zhang, J.: Stability analysis of hydro-turbine governing system including surge tanks under interconnected operation during small load disturbance. Renewable Energy 133, 1426–1435 (2019)
7. Vournas, C., Papaioannou, G.: Modelling and stability of a hydro plant with two surge tanks. IEEE Trans. Energy Convers. 10(2), 368–375 (1995)
8. A.Kuriqi, A. N. Pinheiro, A.Sordo-Ward, L. Garrote: Water-energy-ecosystem nexus: balancing competing interests at a run-of-river hydropower plant coupling a hydrologic–ecohydraulic approach. Energy Convers. Manage. 223, 113267 (2020)
9. Choi, Y.J., Oh, B.C., Acquah, M.A., Kim, D.M., Kim, S.Y.: Optimal operation of a hybrid power system as an island microgrid in south-korea. Sustainability 13(9), 5022 (2021)
10. Jiang, C., Ma, Y., Wang, C.: PID controller parameters optimization of hydro-turbine governing systems using deterministic-chaotic-mutation evolutionary programming (DCMEP). Energy Convers. Manage. 47(9–10), 1222–1230 (2006)
11. Laghari, J.A., Mokhlis, H., Bakar, A., Halim, A., Mohamad, H.: A fuzzy based load frequency control for distribution network connected with mini hydro power plant. J. Intell. Fuzzy Syst. 26(3), 1301–1310 (2014)
12. Parmar, K.S., Majhi, S., Kothari, D.: Load frequency control of a realistic power system with multi-source power generation. Int. J. Electr. Power Energy Syst. 42(1), 426–433 (2012)
13. Zhao, X., Zong, Q., Tian, B., You, M.: Finite-time dynamic allocation and control in multiagent coordination for target tracking. IEEE Trans. Cybern. 52(3), 1872–1880 (2022)
14. Zhou, C., Liu, X., Xu, F., Chen, W.: Sliding mode switch control of adjustable hydro-pneumatic suspension based on parallel adaptive clonal selection algorithm. Appl. Sci. 10(5), 1852 (2020)
15. Yang, T., Wang, B., Chen, P.: Design of a finite-time terminal sliding mode controller for a nonlinear hydro-turbine governing system. Energies 13(3), 634 (2020)
16. Wu, F., Li, F., Chen, P., Wang, B.: Finite-time control for a fractional-order non-linear HTGS. IET Renewable Power Gener. 13(4), 633–639 (2019)
17. Nayak, J.R., Shaw, B., Sahu, B.K.: Implementation of hybrid SSA–SA based three-degree-of-freedom fractional-order PID controller for AGC of a two-area power system integrated with small hydro plants. IET Gener. Transm. Distrib. 14(13), 2430–2440 (2020)
18. Chen, C., Huang, J., Wu, D., Tu, X.: Interval type-2 fuzzy disturbance observer-based T–S fuzzy control for a pneumatic flexible joint. IEEE Trans. Ind. Electron. 69(6), 5962–5972 (2022)
19. Park, I.S., Kwon, N.K., Park, P.: Dynamic output-feedback control for singular T–S fuzzy systems using fuzzy Lyapunov functions. Nonlinear Dyn. 98(3), 1957–1971 (2019)
20. Sun, X., Zhang, H., Cai, Y., Wang, S., Chen, L.: Hybrid modeling and predictive control of intelligent vehicle longitudinal velocity considering nonlinear tire dynamics. Nonlinear Dyn. 97(2), 1051–1066 (2019)
21. Chen, C., Huang, J., Wu, D., Tu, X.: Interval type-2 fuzzy disturbance observer-based T–S fuzzy control for a pneumatic flexible joint. IEEE Trans. Ind. Electron. 69(6), 5962–5972 (2022)
22. Huang, Y., Wu, F.: Finite-time passivity and synchronization of coupled complex-valued memristive neural networks. Inf. Sci. 580, 775–800 (2021)
23. Bhat, S.P., Bernstein, D.S.: Continuous finite-time stabilization of the translational and rotational double integrators. IEEE Trans. Autom. Control 43(5), 678–682 (1998)
24. Liu, Y., Li, H., Zuo, Z., Li, X., Lu, R.: An overview of finite/fixed-time control and its application in engineering systems. IEEE/CAA J. Autom. Sin. PP(9), 1–15 (2022)
25. Ai, Q., Liu, T., Yin, Y., Tao, Y.: Frequency coordinated control strategy of HVDC sending system with wind power based on situation awareness. IET Gener. Transm. Distrib. 14(16), 3179–3186 (2020)
26. Wang, J., Ji, Z., Xu, H., Qiu, J., Jiang, Y.: Finite-time sampled-data H_∞ control of markovian jumping linear systems with mode-dependent time-varying delays. Optim. Control Appl. Methods 43(3), 787–803 (2022)

27. Wang, R., Xing, J., Xiang, Z.: Finite-time asynchronous control of linear time-varying switched systems. Int. J. Adapt Control Signal Process. 35(9), 1824–1841 (2021)
28. Guo, Z., Wang, Z., Li, S.: Global finite-time set stabilization of spacecraft attitude with disturbances using second-order sliding mode control. Nonlinear Dyn. 108(2), 1305–1318 (2022)
29. Yu, M., Song, C., Lv, F., Jin, K., Tan, W.: Event-triggered consensus approach for distributed battery energy storage systems. IET Gener. Transm. Distrib. 13(22), 5102–5108 (2019)
30. Wang, F., Chen, B., Lin, C., Zhang, J., Meng, X.: Adaptive neural network finite-time output feedback control of quantized nonlinear systems. IEEE Trans. Cybern. 48(6), 1839–1848 (2018)
31. Fakharizade Bafghi, H., Jahed.Motlagh, M.R., Abooee, A., Moarefianpur, A.: Robust finite-time tracking for a square fully actuated class of nonlinear systems. Nonlinear Dyn. 103(2), 1611–1625 (2021)
32. Song, X., Wang, M., Ahn, C.K., Song, S.: Finite-time H_∞ asynchronous control for nonlinear Markov jump distributed parameter systems via quantized fuzzy output-feedback approach. IEEE Trans. Cybern. 50(9), 4098–4109 (2020)
33. Gu, Y., Shen, M., Ren, Y., Liu, H.: h_∞ finite-time control of unknown uncertain systems with actuator failure. Appl. Math. Comput. 383, 125375 (2020)
34. Sun, K., Liu, L., Qiu, J., Feng, G.: Fuzzy adaptive finite-time fault-tolerant control for strict-feedback nonlinear systems. IEEE Trans. Fuzzy Syst. 29(4), 786–796 (2020)
35. Sun, K., Qiu, J., Karimi, H.: Neural adaptive fault-tolerant finite-time control for nonstrict feedback systems: an event-triggered mechanism. Neural Networks 143, 377–385 (2021)
36. Ai, Y., Wang, H.: Fixed-time anti-synchronization of unified chaotic systems via adaptive backstepping approach. IEEE Trans. Circuits Syst. II Express Briefs 1–1 (2022). https://doi.org/10.1109/TCSII.2022.3179377
37. Ma, J., Wang, H., Qiao, J.: Adaptive neural fixed-time tracking control for high-order nonlinear systems. IEEE Trans. Neural Networks Learn. Syst. 1–10 (2022). https://doi.org/10.1109/TNNLS.2022.3176625
38. Cheng, P., He, S., Luan, X., Liu, F.: Finite-region asynchronous h_∞ control for 2D Markov jump systems. Automatica 129, 109590 (2021)
39. He, S., Lyu, W., Liu, F.: Robust h_∞ sliding mode controller design of a class of time-delayed discrete conic-type nonlinear systems. IEEE Trans. Syst., Man, Cybern.: Syst. 51(2), 885–892 (2021)
40. Cheng, P., He, S., Cheng, J., Luan, X., Liu, F.: Asynchronous output feedback control for a class of conic-type nonlinear hidden Markov jump systems within a finite-time interval. IEEE Trans. Syst., Man, Cybern.: Syst. 51(12), 7644–7651 (2021)
41. Shi, X.N., Zhou, Z.G., Zhou, D., Li, R.: Event-triggered fixed-time adaptive trajectory tracking for a class of uncertain nonlinear systems with input saturation. IEEE Trans. Circuits Syst. II Express Briefs 68(3), 983–987 (2021)
42. Fang, L., Ma, L., Ding, S., Park, J.H.: Finite-time stabilization of high-order stochastic nonlinear systems with asymmetric output constraints. IEEE Trans. Syst., Man, Cybern.: Syst. 51(11), 7201–7213 (2020)
43. Bhat, S.P., Bernstein, D.S.: Finite-time stability of continuous autonomous systems. SIAM J. Control Optim. 38(3), 751–766 (2000)
44. Polyakov, A.: Nonlinear feedback design for fixed-time stabilization of linear control systems. IEEE Trans. Autom. Control 57(8), 2106–2110 (2012)
45. Hardy, G.H., Littlewood, J.E., Pólya, G.: Inequalities. Cambridge University Press, Cambridge, United Kingdom (1952)
46. Kuczma, M.: An introduction to the theory of functional equations and inequalities: Cauchy's equation and Jensen's inequality. Springer, Berlin, Heidelberg (2009)
47. Rapp, B.E.: Microfluidics: Modeling, Mechanics and Mathematics. William Andrew, Norwich, NY (2016)
48. Yu, X., Feng, Y., Man, Z.: Terminal sliding mode control – an overview. IEEE Open J. Ind. Electron. Soc. 2, 36–52 (2021)
49. Xu, B., Chen, D., Zhang, H., Wang, F.: Modeling and stability analysis of a fractional-order Francis hydro-turbine governing system. Chaos, Solitons Fractals 75, 50–61 (2015)
50. Zhang, R., Chen, D., Ma, X.: Nonlinear predictive control of a hydropower system model. Entropy 17(9), 6129–6149 (2015)

How to cite this article: Zhang, R., Ren, X., Mahmud, M.A., Li, H.: Nonlinear finite-time control of hydroelectric systems via a novel sliding mode method. IET Gener. Transm. Distrib. 1–10 (2022). https://doi.org/10.1049/gtd2.12660

APPENDIX A: PROOF OF THEOREMS

Proof of Theorem 1 The finite stability of the controlled system (4) will be proved through the Lyapunov theorem. First of all, we should prove that the controller (10) enables the sliding surface (6) to reach within a finite settling time. A Lyapunov function for the sliding surface is selected as:

$$L = \frac{1}{2}\mathbf{S}^T\mathbf{S} \geq 0 \tag{A1}$$

The differentiation of Lyapunov function (A1) can be written as:

$$\begin{aligned}\dot{L} &= \mathbf{S}^T\dot{\mathbf{S}} = \sum_{i=1}^{n} s_i\dot{s}_i \\ &= -\sum_{i=1}^{n} s_i\left[\varepsilon sgn(s_i)|s_i|^{2-\beta} + \zeta sgn(s_i)|s_i| \right. \\ &\quad \left. + \sigma sgn(s_i)|s_i|^{\beta}\right] \\ &= -\sum_{i=1}^{n}\left[\varepsilon sign^2(s_i)|s_i|^{3-\beta} + \zeta sign^2(s_i)|s_i|^2 \right. \\ &\quad \left. + \sigma sign^2(s_i)|s_i|^{\beta+1}\right],\end{aligned} \tag{A2}$$

where $i = 1, 2, \ldots, n$. If the sliding surface has reached to the origin, there are $\mathbf{S} = \mathbf{0}$, and $\dot{L} = 0$. Therefore, the derivative of Lyapunov function (A1) can be further rewritten as:

$$\dot{L} = -\sum_{i=1}^{n}\left(\varepsilon|s_i|^{3-\beta} + \zeta|s_i|^2 + \sigma|s_i|^{\beta+1}\right). \tag{A3}$$

In accordance with *Lemma* 1 and 2, one can get:

$$\begin{aligned}\dot{L} &= -\sum_{i=1}^{n}\left(\varepsilon|s_i|^{\frac{3-\beta}{2}} + \zeta|s_i|^2 + \sigma|s_i|^{\frac{\beta+1}{2}}\right) \\ &\leq -\frac{\varepsilon}{n^{\frac{1-\beta}{2}}}\|s_i\|_2^{3-\beta} - \zeta\|s_i\|_2^2 - \sigma\|s_i\|_2^{\beta+1} \\ &= -\frac{\varepsilon}{n^{\frac{1-\beta}{2}}}(2L)^{\frac{3-\beta}{2}} - \zeta(2L) - \sigma(2L)^{\frac{\beta+1}{2}}.\end{aligned} \tag{A4}$$

The left part of Equation (A4) is rewritten as:

$$\begin{aligned}\frac{dL}{dt} &\le -\frac{\varepsilon}{n^{\frac{1-\beta}{2}}}(2L)^{\frac{3-\beta}{2}} - \zeta(2L) - \sigma(2L)^{\frac{\beta+1}{2}} \\ &= -(2L)^{\frac{\beta+1}{2}}\left(\frac{\varepsilon}{n^{\frac{1-\beta}{2}}}(2L)^{1-\beta} + \zeta(2L)^{\frac{1-\beta}{2}} + \sigma\right).\end{aligned} \tag{A5}$$

Since the following to inequalities hold:

$$\begin{aligned}&\frac{(2L)^{-\frac{\beta+1}{2}}dL}{dt} \le -\left(\frac{\varepsilon}{n^{\frac{1-\beta}{2}}}(2L)^{1-\beta} + \zeta(2L)^{\frac{1-\beta}{2}} + \sigma\right); \\ &\frac{\frac{1}{1-\beta}d\left((2L)^{\frac{1-\beta}{2}}\right)}{dt} \le -\left(\frac{\varepsilon}{n^{\frac{1-\beta}{2}}}(2L)^{1-\beta} + \zeta(2L)^{\frac{1-\beta}{2}} + \sigma\right).\end{aligned} \tag{A6}$$

The following inequality can be obtained:

$$dt \le \frac{\frac{1}{1-\beta}d\left((2L)^{\frac{1-\beta}{2}}\right)}{-\left(\frac{\varepsilon}{n^{\frac{1-\beta}{2}}}(2L)^{1-\beta} + \zeta(2L)^{\frac{1-\beta}{2}} + \sigma\right)}. \tag{A7}$$

Integrating both sides of Equation (A7) from t_0 to t_s, where t_0 is the initial time, and at t_s, $L(t_s) = 0$ is hold, the following equation can be obtained:

$$\int_{t_0}^{t_s} dt \le \int_{(2L(t_0))^{\frac{1-\beta}{2}}}^{(2L(t_s))^{\frac{1-\beta}{2}}} \frac{-\frac{1}{1-\beta}}{\left(\frac{\varepsilon}{n^{\frac{1-\beta}{2}}}(2L)^{1-\beta} + \zeta(2L)^{\frac{1-\beta}{2}} + \sigma\right)} d\left((2L)^{\frac{1-\beta}{2}}\right), \tag{A8}$$

where t_0 to t_s are the initial and settling time of the surface, respectively. Here if $\zeta^2 < 4\sigma\varepsilon n^{-\frac{1-\beta}{2}}$, the result in Equation (A8) will be as:

$$\begin{aligned}t_s - t_0 \le{}& \frac{2}{(1-\beta)\sqrt{4\sigma\varepsilon n^{-\frac{1-\beta}{2}} - \zeta^2}} \arctan \\ &\frac{2\varepsilon n^{-\frac{1-\beta}{2}}(2L(t_0))^{\frac{1-\beta}{2}} + \zeta}{\sqrt{4\varepsilon\sigma n^{-\frac{1-\beta}{2}} - \zeta^2}} \\ &- \frac{2}{(1-\beta)\sqrt{4\sigma\varepsilon n^{-\frac{1-\beta}{2}} - \zeta^2}} \arctan \\ &\frac{2\varepsilon n^{-\frac{1-\beta}{2}}(2L(t_s))^{\frac{1-\beta}{2}} + \zeta}{\sqrt{4\varepsilon\sigma n^{-\frac{1-\beta}{2}} - \zeta^2}},\end{aligned} \tag{A9}$$

Assume that $t_0 = 0$ and the sliding surface reaches 0, which is $L(t_s) = 0$. Equation (A9) can be respectively written as:

$$t_s \le \frac{2}{(1-\beta)\sqrt{4\sigma\varepsilon n^{-\frac{1-\beta}{2}} - \zeta^2}} \arctan \frac{2\varepsilon n^{-\frac{1-\beta}{2}}(2L(t_0))^{\frac{1-\beta}{2}} + \zeta}{\sqrt{4\varepsilon\sigma n^{-\frac{1-\beta}{2}} - \zeta^2}}. \tag{A10}$$

On the contrary, if $\zeta^2 \ge 4\sigma\varepsilon n^{-\frac{1-\beta}{2}}$, Equation (A8) results $t_s \le 0$ which is unrealistic. Thus, $\zeta^2 < 4\sigma\varepsilon n^{-\frac{1-\beta}{2}}$ must be satisfied. Form Equation (A10), the finite settling time of sliding surface depends on the initial values. Secondly, the finite stability of the controlled system can also be proved by the Lyapunov theorem. We can structure the following Lyapunov function:

$$V = \frac{1}{2}\mathbf{e}^T\mathbf{e} \ge 0. \tag{A11}$$

From Equation (A10), the sliding surface has reached 0 at t_s. Thus from Equation (6), the sliding surface $\mathbf{S}$ and system error $\mathbf{e}$ are:

$$\begin{aligned}&\mathbf{S} = \mathbf{e} + \eta\mathbf{sgn}(\mathbf{e})\int_{t_0}^{t}\left(\sum_{i=1}^{n}|e_i|^{2\alpha} + 1\right)^{\frac{3}{2}}\sum_{i=1}^{n}|e_i|^{1-\alpha}d\tau = \mathbf{0}, \\ &\mathbf{e} = -\eta\mathbf{sgn}(\mathbf{e})\int_{t_0}^{t}\left(\sum_{i=1}^{n}|e_i|^{2\alpha} + 1\right)^{\frac{3}{2}}\sum_{i=1}^{n}|e_i|^{1-\alpha}d\tau.\end{aligned} \tag{A12}$$

The derivative of Equation (A12) is shown as Equation (A13).

$$\begin{aligned}\dot{\mathbf{e}} = {}& -\eta\mathbf{sgn}(\mathbf{e})\left(\sum_{i=1}^{n}|e_i|^{2\alpha} + 1\right)^{\frac{3}{2}}\sum_{i=1}^{n}|e_i|^{1-\alpha} \\ &-\eta\mathbf{ffi}(\mathbf{e})\int_{t_0}^{t}\left(\sum_{i=1}^{n}|e_i|^{2\alpha} + 1\right)^{\frac{3}{2}}\sum_{i=1}^{n}|e_i|^{1-\alpha}d\tau.\end{aligned} \tag{A13}$$

Also, substituting Equation (A13) into the derivative of Equation (A11) gives:

$$\begin{aligned}\dot{V} &= \mathbf{e}^T\dot{\mathbf{e}} \\ &= -\mathbf{e}^T\begin{pmatrix}\eta\mathbf{sgn}(\mathbf{e})\left(\sum_{i=1}^{n}|e_i|^{2\alpha} + 1\right)^{\frac{3}{2}}\sum_{i=1}^{n}|e_i|^{1-\alpha} \\ -2\eta\boldsymbol{\delta}(\mathbf{e})\int_{t_0}^{t}\left(\sum_{i=1}^{n}|e_i|^{2\alpha} + 1\right)^{\frac{3}{2}}\sum_{i=1}^{n}|e_i|^{1-\alpha}d\tau\end{pmatrix} \\ &= -\mathbf{e}^T\eta\mathbf{sgn}(\mathbf{e})\left(\sum_{i=1}^{n}|e_i|^{2\alpha} + 1\right)^{\frac{3}{2}}\sum_{i=1}^{n}|e_i|^{1-\alpha} \\ &\le -\sum_{i=1}^{n}\left(\lambda|e_i|\mathrm{sgn}^2(e_i)\left(\sum_{i=1}^{n}|e_i|^{2\alpha} + 1\right)^{\frac{3}{2}}\sum_{i=1}^{n}|e_i|^{1-\alpha}\right),\end{aligned} \tag{A14}$$

where $\lambda = \min\{\lambda_i\}$, and $\lambda_i = eigenvalue(\eta)$. Equation (A14) results from $\mathbf{e}^T\boldsymbol{\delta}(\mathbf{e}) = \mathbf{0}$ and Equation (A14) can be rewritten as:

$$\dot{V} \le -\lambda \sum_{i=1}^{n} |e_i| \left(\sum_{i=1}^{n} |e_i|^{2\alpha} + 1 \right)^{\frac{3}{2}} \sum_{i=1}^{n} |e_i|^{1-\alpha}. \tag{A15}$$

The implementation of *Lemma* 1 on Equation (A15) gives:

$$\begin{aligned} \dot{V} &\le -\lambda \left(\sum_{i=1}^{n} |e_i|^2 \right)^{\frac{2-\alpha}{2}} \left(\left(\sum_{i=1}^{n} |e_i|^2 \right)^{\alpha} + 1 \right)^{\frac{3}{2}} \\ &= -\lambda (2V)^{\frac{2-\alpha}{2}} \left((2V)^{\alpha} + 1 \right)^{\frac{3}{2}}. \end{aligned} \tag{A16}$$

The left hand side of Equation (A16) can be rewritten as:

$$\begin{aligned} \frac{dV}{dt} &\le -\lambda (2V)^{\frac{2-\alpha}{2}} \left((2V)^{\alpha} + 1 \right)^{\frac{3}{2}}, \\ dt &\le -\frac{dV}{\lambda (2V)^{\frac{2-\alpha}{2}} \left((2V)^{\alpha} + 1 \right)^{\frac{3}{2}}}, \\ dt &\le -\frac{1}{\lambda\alpha} \frac{1}{\sqrt{\left((2V)^{\alpha} + 1 \right)^3}} d(2V)^{\frac{\alpha}{2}}. \end{aligned} \tag{A17}$$

Integrating Equation (A17) from t_s to $t_\varkappa$ gives:

$$\begin{aligned} \int_{t_s}^{t_\varkappa} dt &\le -\int_{(2V(t_s))^{\frac{\alpha}{2}}}^{(2V(t_\varkappa))^{\frac{\alpha}{2}}} \frac{1}{\lambda\alpha} \frac{1}{\sqrt{\left((2V)^{\alpha} + 1 \right)^3}} d(2V)^{\frac{\alpha}{2}}, \\ t_\varkappa - t_s &\le \frac{1}{\lambda\alpha} \left(\frac{(2V(t_s))^{\frac{\alpha}{2}}}{\sqrt{(2V(t_s))^{\alpha} + 1}} - \frac{(2V(t_\varkappa))^{\frac{\alpha}{2}}}{\sqrt{(2V(t_\varkappa))^{\alpha} + 1}} \right), \end{aligned} \tag{A18}$$

where at $t_\varkappa$, there is $V(t_\varkappa) = 0$. When $V(t_\varkappa) = 0$, the system reaches the reference within a finite settling time. Thus, Equation (A18) is written as:

$$t_\varkappa - t_s \le \frac{1}{\eta\alpha} \frac{(2V(t_s))^{\frac{\alpha}{2}}}{\sqrt{(2V(t_s))^{\alpha} + 1}}. \tag{A19}$$

When $\zeta^2 < 4\sigma\varepsilon n^{-\frac{1-\beta}{2}}$ is satisfied, the controlled system can reach the reference within the finite settling time $T_\varkappa$ in Equation (14).

Proof of Theorem 2 Since $\arctan(\cdot)$ is bounded and

$$\begin{aligned} \frac{(2V(t_s))^{\frac{\alpha}{2}}}{\sqrt{(2V(t_s))^{\alpha} + 1}} &\le 1, \\ \arctan \frac{2\varepsilon n^{-\frac{1-\beta}{2}} (2L(t_0))^{\frac{1-\beta}{2}} + \zeta}{\sqrt{4\varepsilon\sigma n^{-\frac{1-\beta}{2}} - \zeta^2}} &< \frac{\pi}{2}, \end{aligned} \tag{A20}$$

the maximum of Equation (14) is Equation (15).